

ROCA ET AL., MESOZOIC ORIGIN FOR WEST INDIAN INSECTIVORES

SUPPLEMENTARY INFORMATION

Detailed Materials and Methods	Page 2
Suppl. Table 1 Samples of <i>Solenodon cubanus</i>	Page 3
Suppl. Table 2 Primers for <i>Solenodon cubanus</i>	Page 5
Suppl. Figure 1 <i>Solenodon paradoxus</i> relationship to other mammals	Page 8
Suppl. Table 3 Phylogenetic support for <i>Solenodon</i> position	Page 10
Suppl. Figure 2 Molecular divergence date estimates	Page 13
Suppl. Figure 3 Relationship of <i>Solenodon</i> to fossil insectivores	Page 15
Suppl. Figure 4 Divergence estimates for <i>Cricosaura typica</i>	Page 17
References for Supplementary Information	Page 20

## SUPPLEMENTARY DOCUMENT: DETAILED MATERIALS AND METHODS.

*Solenodon paradoxus: Extraction, Amplification and Sequencing*

*Solenodon paradoxus* DNA was extracted from a fresh blood sample using a column-based kit (Qiagen). DNA was amplified and sequenced to generate a concatenated dataset of 16 nuclear gene segments (*ADORA3*, *ADRA2B*, *ADRB2*, *APP*, *ATP7A*, *BDNF*, *BMI1*, *BRCA1*, *CREM*, *EDG1*, *PLCB4*, *RAG1*, *RAG2*, *TYR*, *VWF*, *ZFX*) and the two nearly complete mitochondrial rRNA subunit genes (12S and 16S) with the intervening gene for valine tRNA<sup>1</sup>. Nucleotide sequences for *Solenodon paradoxus* were obtained using previously described PCR primers<sup>2,3</sup>. Sequences were collected on ABI 3700 and 3730 automated sequencers (ABI) using BigDye terminator chemistry (ABI). Alignments were based on those previously published<sup>1</sup>, modified as required to include the new taxon. All regions for which reliable homology could not be established were removed from the analyses, resulting in a 13,885 bp data set.

*Solenodon cubanus: Extraction, Amplification and Sequencing*

Individuals of *S. cubanus* are only very rarely caught, and the species had been considered extinct at various times during the past century<sup>4</sup>. Thus for *S. cubanus* only museum samples were available. The five museum tissue specimens sampled for this study are listed in Supplementary Table 1. Samples of tissue, *circa* 0.4 cm<sup>3</sup> were prepared in a physically isolated ancient DNA laboratory. Samples from the Museum für Naturkunde (Berlin) had been stored in ethanol and were therefore dried overnight

Supplementary Table 1: Samples of *Solenodon cubanus*

Lab. of Genomic Diversity number	Label	Museum* and specimen no.	Sex and age	Sample type†	Collection info.‡
Scu-MCZ12413	S1	MCZ 12413	Male, Adult	Tissue from untanned? skin	F. Poey? 1850-1855?
Scu-MFN3344	Sa	MFN 3344	Male, Adult	Abdominal muscle (alcohol)	F. Poey, 19th century
Scu-MFN3320	Sj	MFN 3320	Male, Juvenile	Abdominal muscle (alcohol)	Gundlach, 19th century
Scu-MCZ46305	S2	MCZ 46305	Unknown	Dried snout tissue from skull	Grandidier Collection, pre-1947
Scu-MCZ3223	S3	MCZ 3223	Male, Adult	Skin, urogenital (alcohol)	G. A. Maack, 1871

\*MCZ: Museum of Comparative Zoology, Harvard University, Cambridge MA, USA

\*MFN: Museum für Naturkunde, Humboldt-Universität zu Berlin, Germany

†Scu-MCZ3223 was a mounted skin from a specimen that had been in alcohol, thus it may have been formalin-exposed.

‡Scu-MCZ12413 collection information is based on Barbour 1944 (Proc. New England Zool. Club 23:1-8).

prior to extraction. DNA was extracted from all of the tissues as previously described<sup>5,6</sup>, using guanidine thiocyanate (GuHCL)<sup>7</sup> and silica-based purification<sup>8</sup> methods. DNA extraction and pre-amplification steps for PCR were carried out in a dedicated laboratory for ancient DNA studies, which was physically isolated from the Laboratory of Genomic Diversity, with separate pipettes, disposable sterile tubes, filter tips, sterile reagents and solutions used throughout the procedures. DNA extractions and PCR setups were performed in separate ultraviolet-exposed hoods to prevent contamination by contemporary DNA. All reagents and tubes were irradiated with ultraviolet light to minimize contamination by contemporary DNA. Multiple negative extraction and amplification controls were included with each amplification to detect contamination. The longest total sequence was obtained for Scu-MCZ12413; the authenticity of sequences produced by 13 of 19 primer pairs (see below) was verified using another sample, Scu-MFN3344, which was extracted in a different building, and which had sequences identical to Scu-MCZ12413. For a minority of the sequences the authenticity was also supported by multiple extractions of Scu-MCZ12413 performed in separate rooms, or by sequences from a third individual, Scu-MFN3320, which differed from the other two individuals by a single nucleotide difference. Thus the authenticity of the sequence for *Solenodon cubanus* was supported using multiple individuals and multiple extractions carried out in different isolated buildings, while the presence of a single nucleotide difference across three individuals may suggest low genetic diversity among *S. cubanus*.

PCR amplification was conducted using high-fidelity Taq-Gold (ABI) to minimize polymerase error. Nineteen pairs of primers were used to amplify overlapping segments of the 12S and 16S mitochondrial ribosomal genes (Supplementary Table 2). We obtained a nearly complete sequence of this mtDNA

Supplementary Table 2: Primers for *Solenodon cubanus* mtDNA, with positions relative to human mtDNA reference NC\_001807.

Primer pair	Start (human)	Forward	Reverse	Start (human)	Reverse	<i>S. cubanus</i> product size
1	603	GCAATGCACTGAAAATGCTTAG	GTTTCCCGTGGGGTGTG	817	GTTTCCCGTGGGGTGTG	230
2	889	GTGCCAGCCACCGGGTCA	TGGGGTATCTAATCCCAGTTTG	1089	TGGGGTATCTAATCCCAGTTTG	200
3	1074	GGGATTAGATACCCCACTATGC	TTGCTGAAGATGGCGGTATA	1278	TTGCTGAAGATGGCGGTATA	209
4	1258	ATATACCGCCATCTTCAGCA	GAGGGTGACGGGCGGTGT	1499	GAGGGTGACGGGCGGTGT	250
5	1319	AAAGACGTTAGGTCAAGGTGT	TGCTTACCATGTTACGACTT	1578	TGCTTACCATGTTACGACTT	271
6	1847	CCTTCTGCATAATGAGTTAACTAG	TGGACAACCAAGCTATCACCA	2028	TGGACAACCAAGCTATCACCA	163
8	2495	CCTGTTTTACCAAAAACATCACC	AAGCTCCATAGGGTCTTCTCGT	2740	AAGCTCCATAGGGTCTTCTCGT	245
9	2808	TTTTGGTTGGGTGACCT	ATCCAACATCGAGGTCGTAAAC	3000	ATCCAACATCGAGGTCGTAAAC	188
10	3044	TCAACGATTAAGTCTACGTGA	TTAAGGAGAGGATTTGAACCT	3303	TTAAGGAGAGGATTTGAACCT	260
11	754	CAGGTATCAAGCACACTAGTACACG	GGTCTCTTTGGCACGGCTTTA	959	GGTCTCTTTGGCACGGCTTTA	208
12	1003	CAAGTCAACATAAAAAATAAACCCACGA	CCTAACGTATTTGCCGTTTTTCG	1330	CCTAACGTATTTGCCGTTTTTCG	334
13	1494	ACCCTCCTCAAA TACTAACAATACTT	GGATAGCTCGTCTGGTTTCG	1926	GGATAGCTCGTCTGGTTTCG	437
14	2081	TGAAATTGACCTCCCAGTGA	TGGATCAATATGTGATGTTATTTT	2304	TGGATCAATATGTGATGTTATTTT	224
15	1979	TGTGGATAGAGGTGAAAAGCCTA	GGCTGCTTTTAGGCCTACTG	2189	GGCTGCTTTTAGGCCTACTG	211
16	2122	GGCAAAGGATAAAACCTTAAATCA	TGATATAAACTTATGCGTGGAGAA	2350	TGATATAAACTTATGCGTGGAGAA	228
17	2251	GAACACATACTGGACCATTCTATT	TTATTGCATGCCCTGTGTTGG	2449	TTATTGCATGCCCTGTGTTGG	190
18	2327	TCTCCACGCATAAGTTTATATCAGA	ATAGTCACTGGGCAGGCAGT	2561	ATAGTCACTGGGCAGGCAGT	233
19	2934	GGGATAACAGCGCAATCCTA	TTCTTGTCCCTTCGTACTGG	3121	TTCTTGTCCCTTCGTACTGG	196

region (1,624 bp after removing ambiguous regions) for *S. cubanus* using overlapping PCR amplifications. Initially, nine non-overlapping mtDNA fragments were amplified using primers for mtDNA regions conserved across mammals (Supplementary Table 2, pairs 1-6 and 8-10). The other sets of primer pairs were then designed from the *S. cubanus* sequence to span the remaining sequence gaps.

Touchdown PCR for all *S. cubanus* gene segments was performed in a volume of 25  $\mu$ l with initial denaturation at 95°C for 10 min followed by a total of 45 cycles of 15 sec at 94°C, 30 sec annealing for 2 cycles each at 60°C, 58°C, 56°C, 54°C, 52°C, and 35 cycles at 50°C or 48°C, and 45 sec elongation at 72°C, with a final extension of 10 min at 72°C. PCR products were purified using Microcon-50 (Millipore) and sequenced as indicated above for *S. paradoxus*.

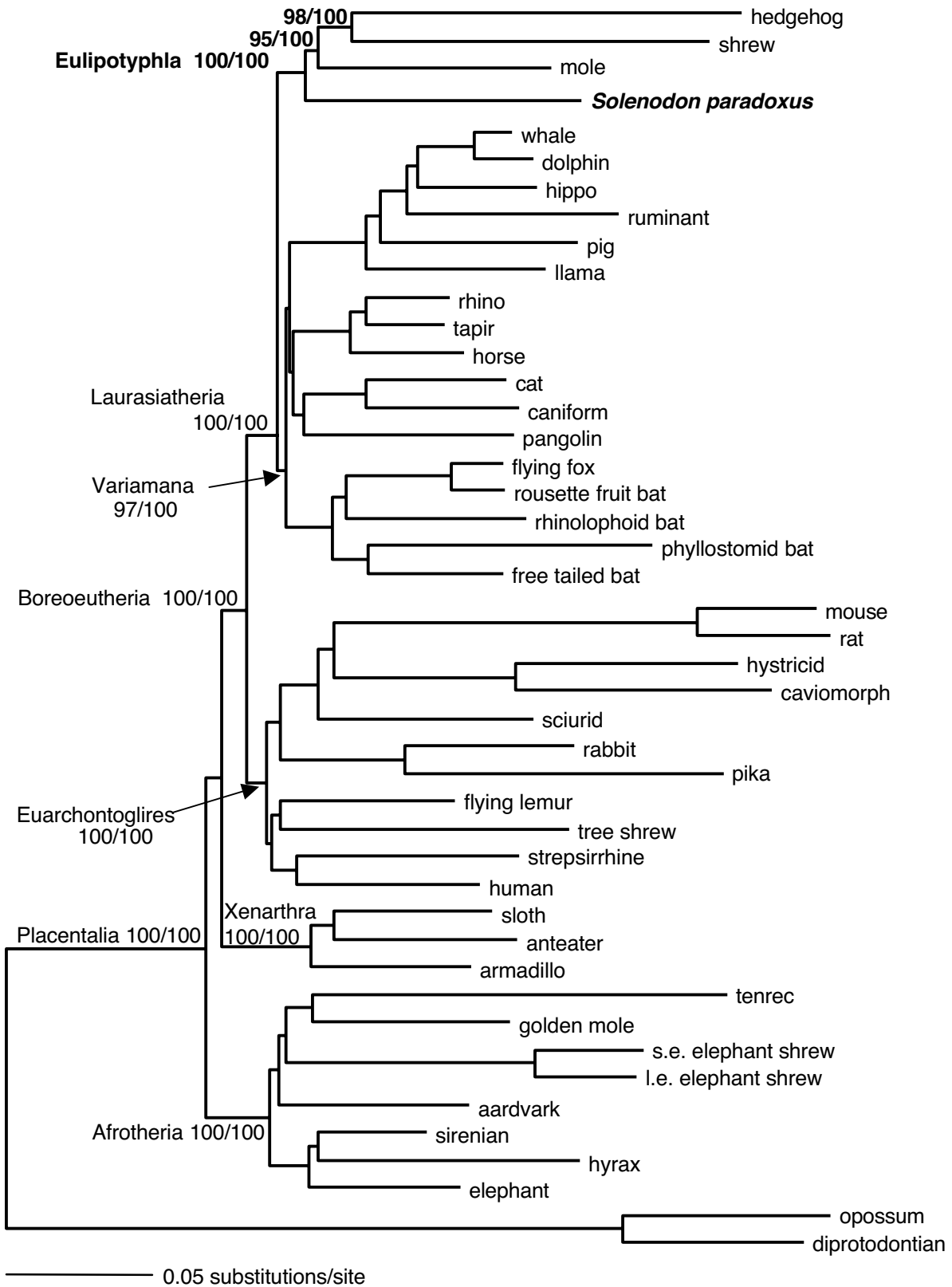
### *Phylogenetic Analyses*

Maximum likelihood (ML) analyses were performed with PAUP\* 4.0b10 (Altivec)<sup>9</sup> and employed heuristic searches using a Neighbor Joining (NJ) starting tree and tree bisection-reconnection (TBR) branch swapping. Nonparametric ML bootstrap analysis was performed using 100 heuristic replicates with nearest neighbor interchange (NNI) branch swapping. Settings for the GTR+ $\Gamma$ +I model of DNA sequence evolution were estimated initially using Modeltest<sup>10</sup> and then optimized using multiple heuristic ML searches in PAUP\*<sup>9</sup> until parameter values stabilized. Parameter settings for the 13.9 kb (after removal of regions of ambiguous homology) combined nuclear+mitochondrial sequence alignment dataset were as follows: R-matrix = (1.292270, 4.672970, 0.891610, 1.261640, 5.328150, 1.0000); base

frequencies: (A=0.2694, C=0.2549, G=0.2383, T=0.2374); proportion of invariant sites = 0.2532; and shape parameter of the gamma distribution = 1.0857.

Supplementary Figure 1 shows the phylogenetic relationship of *Solenodon paradoxus* to other mammals. The tree was generated using 13.9 kb DNA sequence (after removal of ambiguous regions) of nuclear and mitochondrial genes (without the partial *S. cubanus* sequence, see below), using maximum likelihood (ML) methodology (-ln L= 184296.15790) implemented in PAUP\* 4.0b10 (Altimec)<sup>9</sup>; a strongly concordant topology was generated by Bayesian analysis using MrBayes v3.0b4<sup>11</sup> (see below). The major super-ordinal clades, and all clades within Eulipotyphla, are labeled with percent ML bootstrap support (left) and Bayesian posterior probability (BPP) (expressed as a percentage) (right). Minimum evolution (ME) and maximum parsimony (MP) analyses also confirmed the basal position of *Solenodon* within Eulipotyphla (see below).

Supplementary Figure 1: Relationship of *Solenodon paradoxus* to other mammals.



Bayesian phylogenetic analyses were performed using the program MrBayes v3.0b4<sup>11</sup>, as described previously<sup>1</sup>. Performed for each dataset (described below) were two independent runs of 1 million generations, sampling trees every 20 generations, and employing a burnin setting of 100,000 generations. Posterior probabilities for phylogenetic branches and parameters of the model of sequence evolution for the two independent runs were strongly concordant. Additionally, the Bayesian tree generated was almost identical to the ML tree, except for the resolution of Cetartiodactyla *vs.* Perissodactyla *vs.* (Carnivora+Pholidota). ML joined Perissodactyla+(Carnivora+Pholidota), while Bayesian joined Perissodactyla+Cetartiodactyla. These were nodes that had remained unresolved in previous analyses as well<sup>1</sup>.

Phylogenetic support for the position of *Solenodon* is shown on Supplementary Table 3.

Supplementary Table 3. Phylogenetic support for the position of *Solenodon* within Placentalia from multiple phylogenetic methods. Relevant nodes are shown (see Supplementary Figure 1). BAYES=Bayesian posterior probability, ML=maximum likelihood bootstrap, ME=minimum evolution bootstrap, MP=maximum parsimony bootstrap. One hundred bootstrap replicates were performed, with tree bisection reconnection branch swapping (nearest neighbor interchange for the ML run) on a neighbor-joining determined starting tree (run with ML distances and estimated parameters).

CLADE	BAYES-run1	BAYES-run2	ML-GTR+G+I	ME-GTR+G+I	MP
Laurasiatheria	1.00	1.00	100	100	100
Eulipotyphla	1.00	1.00	100	100	100
mole+shrew+hedgehog	1.00	1.00	95	52	82
shrew+hedgehog	1.00	1.00	98	93	95

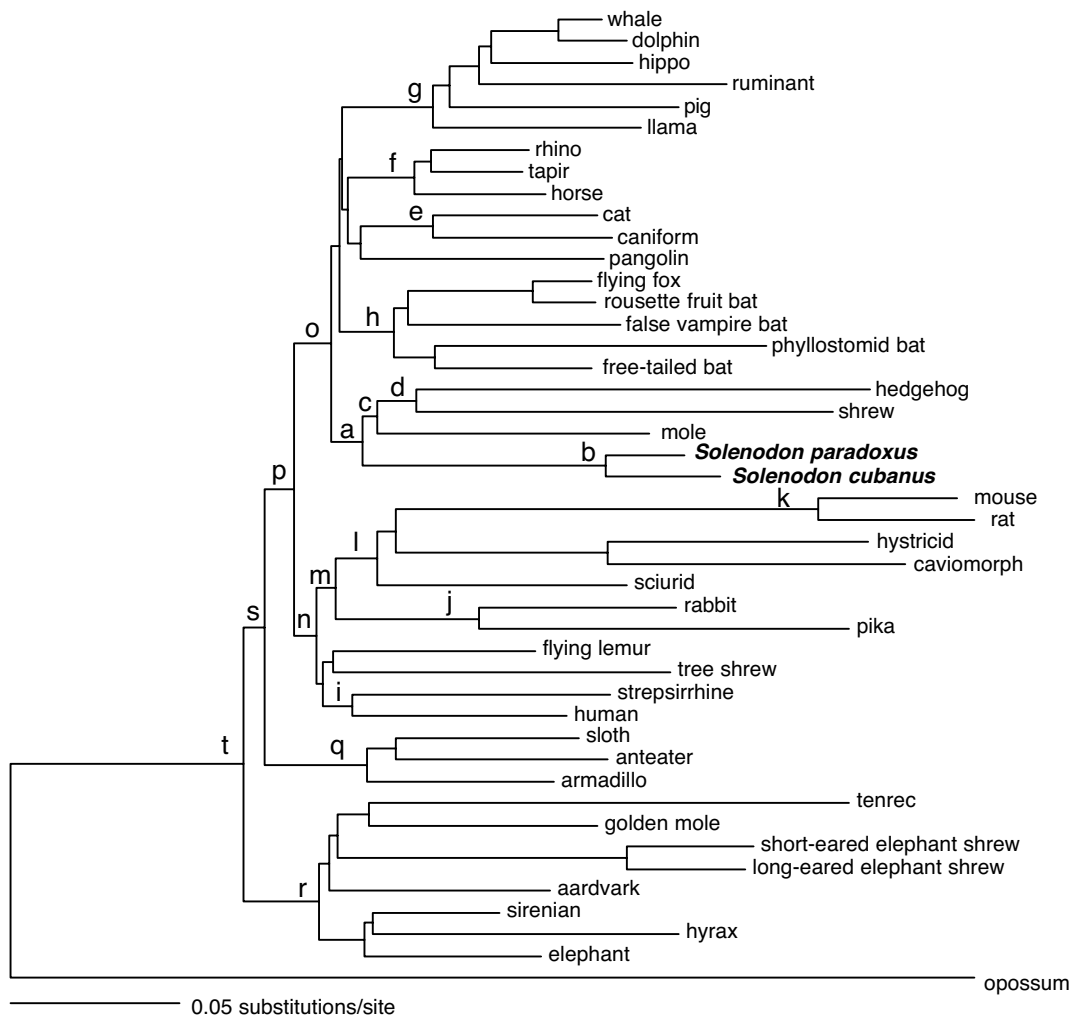
Parameter settings for the 1624 bp (after removal of regions of ambiguous homology) mitochondrial dataset (based on the constrained ML topology of the nuclear+mtDNA dataset) were as follows: R-matrix = (5.13200, 12.73809, 3.55937, 0.60442, 26.20990, 1.0000); base frequencies: (A=0.3457, C=0.2025, G=0.2021, T=0.2496); proportion of invariant sites = 0.4108; and shape parameter of the gamma distribution = 0.5219. Heuristic ML searches (with TBR branch swapping) of the smaller mitochondrial-only dataset were used to identify the phylogenetic position of *S. cubanus*, using the nuclear+mtDNA derived ML topology shown in Supplementary Figure 1 as a backbone phylogenetic constraint. Nonparametric bootstrap analysis was performed as described for the nuclear+mtDNA data set, as was Bayesian analysis. The 1.6 kb mtDNA-only analysis supported a sister relationship between *S. cubanus* and *S. paradoxus* with 100% bootstrap support for ML, MP and ME.

#### *Estimating Divergence Times.*

To estimate divergence times, we employed the Thorne-Kishino method<sup>12,13</sup>, which permits multiple simultaneous constraints from the fossil record while allowing rates of molecular evolution to vary on different branches of a phylogenetic tree. Branch lengths were estimated with the *estbranches* program of Thorne *et al.*<sup>13</sup> for each of three datasets: 1.) nuclear+mtDNA (13.9 kb) with 42 previously sequenced eutherian taxa<sup>1</sup> plus *S. paradoxus*; 2.) nuclear+mtDNA (13.9 kb) with the 42 previous eutherian taxa<sup>1</sup> plus *S. paradoxus* along with mtDNA only (1.6 kb) for *S. cubanus*; 3.) mtDNA only (1.6 kb) with the 42 previous eutherian taxa<sup>1</sup> plus *S. paradoxus* and *S. cubanus*. In each case, we employed the maximum likelihood (ML) tree topology. We used Felsenstein's<sup>14</sup> model of sequence evolution and an allowance for a gamma

distribution of rates with four discrete rate categories. The transition/transversion parameter and estimates of the rate categories of the gamma distribution were estimated with PAUP\*<sup>9</sup> for each data set. Divergence times were estimated using the program *divtime5b*<sup>12,13</sup>. Markov chain Monte Carlo analyses were run for 1 million generations after a burnin of 100,000 generations to allow Markov chains to approach stationarity before states are sampled; chains were sampled every 100 generations. We used 105 million years ago (Mya) as the input value for the mean of the prior distribution of the root of the ingroup tree<sup>15</sup>. We used the following fossil constraints<sup>15</sup> on divergence times: 1.) minimum of 60 Mya for armadillo to sloth/anteater; 2.) minimum of 50 Mya and maximum of 63 Mya for the split between feliform and caniform carnivores; 3.) minimum of 54 Mya and maximum of 58 Mya for the split between hippomorph and ceratomorph perissodactyls; 4.) minimum of 52 Mya for the hippo-cetacean divergence; 5.) maximum of 65 Mya for Cetartiodactyla. 6.) minimum of 54 and maximum of 65 Mya for the base of Paenungulata; 7.) minimum of 12 Mya for *Mus* to *Rattus*; 8.) minimum of 43 Mya and a maximum of 60 Mya for pteropodid bats to the false vampire bat. Molecular divergence dates estimated for select nodes are shown in Supplementary Figure 2. Using instead 65 Mya as the mean of the prior distribution of the root of the ingroup tree, and the nuclear-mitochondrial DNA combined data set, produced an estimate of 76 Mya (72-82 Mya CI) for *Solenodon* versus other eulipotyphlans, and 24 Mya (15-32 Mya CI) for *S. paradoxus* versus *S. cubanus*. Most other nodes change by less than 1 My.

**Supplementary Figure 2.** Molecular divergence dates (Mya) estimated for select nodes within Placentalia based on different molecular data partitions. Nodes are indicated on the ML tree in which *S. cubanus* was placed using a backbone constraint derived from analysis of the entire dataset (see Materials & Methods).



Group	node	mtRNA	Nuclear+mtRNA	Nuclear+mtRNA ( <i>S.paradoxus</i> only)
Base of Eulipotyphla	a	85(75-95)	77(72-82)	76(72-81)
Base of Solenodontidae	b	25(16-38)	23(16-32)	NA
mole-shrew-hedgehog	c	73(61-86)	74(68-79)	73(68-78)
shrew-hedgehog	d	65(51-80)	66(59-72)	65(60-71)
Base of Carnivora	e	54(50-61)	56(51-61)	56(51-61)
Base of Perissodactyla	f	56(54-58)	56(54-58)	56(54-58)
Base of Cetartiodactyla	g	69(60-79)	64(61-67)	63(61-65)
Base of Chiroptera	h	66(58-75)	65(62-67)	64(61-67)
Base of Primates	l	80(67-95)	77(71-84)	77(70-83)
Base of Lagomorpha	j	62(48-77)	51(43-59)	51(43-58)
mouse-rat	k	24(15-36)	15(12-20)	15(12-19)
Base of Rodentia	l	77(64-92)	73(67-80)	73(67-79)
Base of Glires	m	82(70-96)	83(76-90)	82(76-89)
Base of Euarchontoglires	n	90(80-103)	87(81-94)	86(81-93)
Base of Laurasiatheria	o	86(76-96)	84(79-90)	84(79-89)
Base of Boreoeutheria	p	92(81-104)	93(86-101)	92(86-99)
Base of Xenarthra	q	85(70-102)	71(63-79)	70(62-78)
Base of Afrotheria	r	86(74-100)	80(74-86)	80(74-86)
Xenarthra-Boreoeutheria	s	99(86-114)	101(92-110)	100(92-109)
Base of Placentalia	t	102(89-117)	105(96-116)	104(96-114)

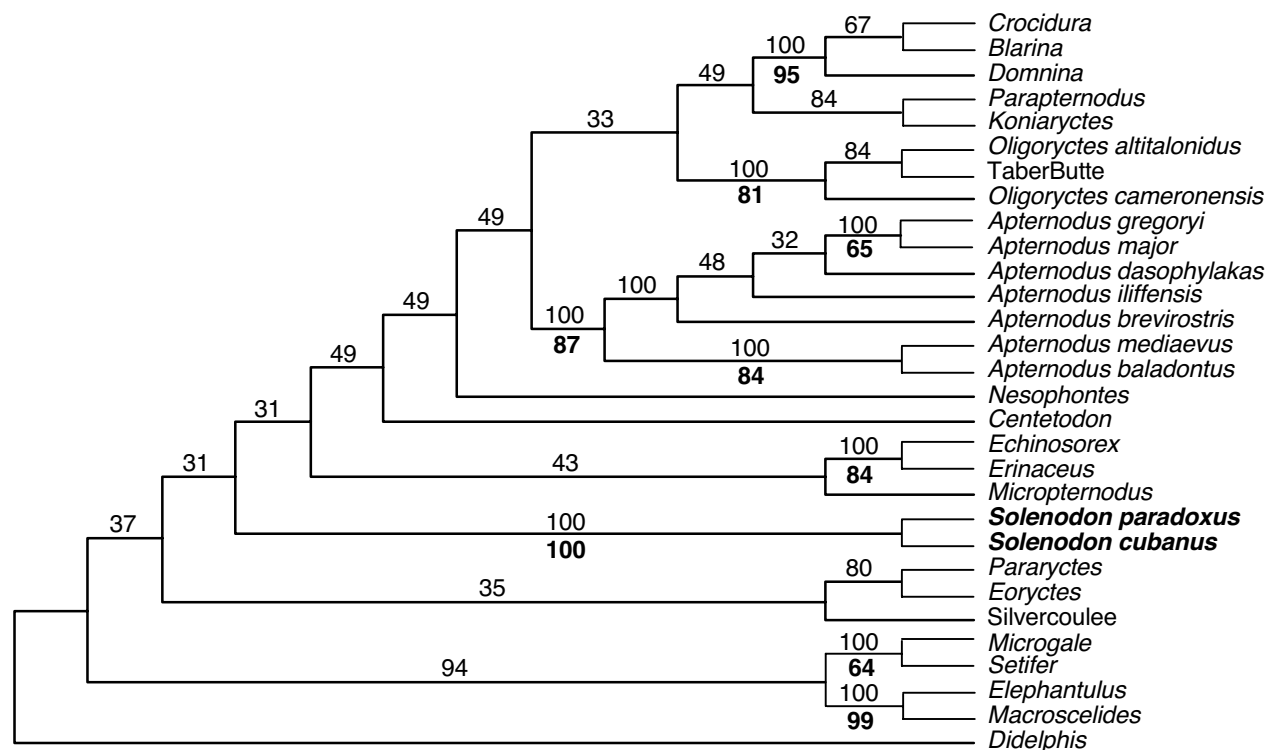
*Relationship of Solenodon to fossil insectivores.*

A parsimony tree was generated based on the morphological dataset of Asher and colleagues (2002)<sup>16</sup>, employing a tree scaffold based on our molecular phylogeny. Results and details of this analysis are shown in Supplementary Figure 3.

**Supplementary Figure 3.** Parsimony tree of living and fossil insectivores based on the morphological data set of Asher et al. (2002)<sup>16</sup> employing the following molecular scaffold (based on the molecular phylogeny presented in the text) as a constraint tree during the phylogenetic analysis, and an opossum as a marsupial outgroup taxon:

*(Didelphis,(((Microgale,Setifer),(Macroscelides,Elephantulus)),((S.paradoxus,S.cubanus),((Echinosorex,Erinaceus),(Crocidura,Blarina))))).*

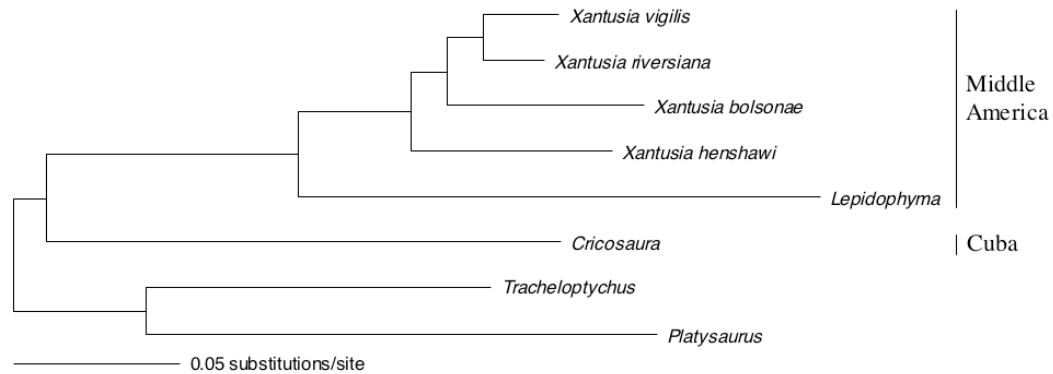
The tree shown is the majority-rule consensus of 295 trees of length 401, with observed bipartitions shown above each branch. The heuristic search employed ordered character transformations (following Asher et al. [2002]<sup>16</sup>), TBR branch swapping and 100 random input orders. Bootstrap proportions  $\geq 50\%$  are in boldface below the branches. The bootstrap search implemented the same heuristic search settings, with the exception that 50 random input orders were used. The molecular scaffold was employed because the parsimony tree of Asher et al. (2002)<sup>16</sup> depicts phylogenetic relationships of extant taxa that are discordant with current molecular phylogenies (i.e. eulipotyphlans and afrosoricids were both paraphyletic in Asher et al. [2002]<sup>16</sup>). The taxa TaberButte and Silvercoulee were informal names for taxa unnamed at the time of publication of Asher et al. (2002)<sup>16</sup>.



*Divergence estimates for Cricosaura typica.*

We employed the Thorne/Kishino method<sup>12,13</sup> to estimate divergence times within the Xantusiidae. Methods and results for this analysis are shown in Supplementary Figure 4.

**Supplementary Figure 4. Divergence estimates for the Cuban lizard *Cricosaura typica* from other mainland xantusiid lizards.**



To estimate the divergence date of the Cuban species *Cricosaura* from the North and Central American genera *Lepidophyma* and *Xantusia*, we utilized the mitochondrial DNA data set of Hedges and colleagues<sup>17,18</sup>. The data set is a concatenation of three gene fragments: 12S rRNA, 16S rRNA and cytochrome b (*cytb*). The analyzed data set was 802 bp after exclusion of ambiguous sites and third positions of the *cytb* gene, because the latter sites begin to saturate at deeper divergences in the tree. We added the outgroup sequences *Tracheloptychus petersi* and *Platysaurus sp.* from Vicario et al. (2003)<sup>19</sup>. ML searches were performed with PAUP\*<sup>9</sup> and employed heuristic searches using an NJ starting tree and TBR branch

swapping. Settings for the GTR+ $\Gamma$ +I model of DNA sequence evolution were estimated initially using Modeltest<sup>10</sup> and then optimized using multiple heuristic ML searches in PAUP\*<sup>9</sup> until parameter values stabilized. Parameter settings for the mitochondrial dataset were as follows: R-matrix = (11.97877, 23.49330, 11.37207, 3.11298, 49.50588, 1.0000); base frequencies = (A= 0.316339, C= 0.234247, G= 0.204491, T= 0.244924); proportion of invariant sites = 0.235564; and shape parameter of the gamma distribution = 0.547144. The resulting maximum likelihood tree (shown above) is identical to the tree found in Hedges et al. (1991)<sup>17</sup> and Hedges & Bezy (1993)<sup>18</sup>, with the Cuban lizard *Cricosaura* being the most basal divergence within Xantusiidae.

We employed the Thorne/Kishino method<sup>12,13</sup> to estimate divergence times within the Xantusiidae. Branch lengths were estimated with *estbranches* given the above topology and employing the F84 model (parameters estimated in PAUP\*<sup>9</sup>), and divergence times were estimated using *divtime5b*. We used the following fossil constraints on divergence times: a minimum of 43 Mya for the split between *Lepidophyma* and *Xantusia* based on two Late Eocene fossil species of “*Paleoxantusia*” that share derived characters with *Lepidophyma* and *Xantusia*, respectively<sup>20</sup>; and a maximum of 60 Mya for the same node<sup>21</sup> based on Middle Paleocene fossils of *Paleoxantusia fera* that share features with both *Lepidophyma* and *Xantusia*, but not *Cricosaura*. Markov chain Monte Carlo analyses were run for 1 million generations after a burnin of 100,000 generations to allow Markov chains to approach stationarity before states are sampled; chains were sampled every 100 generations. We used 65 Mya as the input value for the mean of the prior distribution of the root of the ingroup tree. Analyses varying this prior from 75 Mya to 55 Mya produced similar dates, as follows:

Node	Date with 65 My prior	75 My prior	55 My prior
<i>Cricosaura-Xantusiinae</i>	76(57-101)	78(57-105)	73(55-97)
<i>Lepidophyma-Xantusia</i>	51(43-59)	51(43-59)	50(43-59)
Base of <i>Xantusia</i>	33(22-47)	33(22-47)	33(22-47)

95% credibility intervals are given in parentheses.

## REFERENCES FOR SUPPLEMENTARY MATERIALS

1. Murphy, W. J. et al. Resolution of the early placental mammal radiation using Bayesian phylogenetics. *Science* **294**, 2348-2351 (2001).
2. Murphy, W. J. et al. Molecular phylogenetics and the origins of placental mammals. *Nature* **409**, 614-8 (2001).
3. Madsen, O. et al. Parallel adaptive radiations in two major clades of placental mammals. *Nature* **409**, 610-4 (2001).
4. Fa, J. E. et al. Biodiversity of Sierra del Cristal, Cuba: first insights. *Oryx* **36**, 389-395 (2002).
5. Kahila Bar-Gal, G., Ducos, P. & Kolska Horwitz, L. The application of ancient DNA analysis to identify Neolithic Caprinae: a case study from the site of Hatoula, Israel. *International Journal of Osteoarchaeology* **13**, 120-131 (2003).
6. Kahila Bar-Gal, G., Khalaily, H., Mader, O., Ducos, P. & Kolska Horwitz, L. Ancient DNA evidence for the transition from wild to domestic status in Neolithic goats: a case study from the site of Abu Gosh, Israel. *Ancient Biomolecules* **4**, 9-17 (2002).
7. Boom, R. et al. Rapid and simple method for purification of nucleic acids. *J Clin Microbiol* **28**, 495-503 (1990).
8. Hoss, M. & Paabo, S. DNA extraction from Pleistocene bones by a silica-based purification method. *Nucleic Acids Res* **21**, 3913-4 (1993).
9. Swofford, D. L. *PAUP\*. Phylogenetic Analysis Using Parsimony. Version 4b10*. (Sinauer Associates, Sunderland, Massachusetts, 2003).

10. Posada, D. & Crandall, K. A. MODELTEST: testing the model of DNA substitution. *Bioinformatics* **14**, 817-8 (1998).
11. Huelsenbeck, J. P. & Ronquist, F. MRBAYES: Bayesian inference of phylogenetic trees. *Bioinformatics* **17**, 754-755 (2001).
12. Kishino, H., Thorne, J. L. & Bruno, W. J. Performance of a divergence time estimation method under a probabilistic model of rate evolution. *Mol Biol Evol* **18**, 352-61 (2001).
13. Thorne, J. L., Kishino, H. & Painter, I. S. Estimating the rate of evolution of the rate of molecular evolution. *Mol Biol Evol* **15**, 1647-57 (1998).
14. Felsenstein, J. Distance methods for inferring phylogenies: a justification. *Evolution* **38**, 16-24 (1984).
15. Springer, M. S., Murphy, W. J., Eizirik, E. & O'Brien, S. J. Placental mammal diversification and the Cretaceous-Tertiary boundary. *Proc Natl Acad Sci U S A* **100**, 1056-61 (2003).
16. Asher, R. J., McKenna, M. C., Emry, R. J., Tabrum, A. R. & Kron, D. G. Morphology and relationships of *Apternodus* and other extinct, zalambdodont placental mammals. *Bul. Amer. Mus. Nat. Hist.* **217**, 1-117 (2002).
17. Hedges, S. B., Bezy, R. L. & Maxson, L. R. Phylogenetic relationships and biogeography of xantusiid lizards, inferred from mitochondrial DNA sequences. *Mol Biol Evol* **8**, 767-80 (1991).
18. Hedges, S. B. & Bezy, R. L. Phylogeny of xantusiid lizards: concern for data and analysis. *Mol Phylogenet Evol* **2**, 76-87 (1993).
19. Vicario, S., Caccone, A. & Gauthier, J. Xantusiid "night" lizards: a puzzling phylogenetic problem revisited using likelihood-based Bayesian methods on mtDNA sequences. *Mol Phylogenet Evol* **26**, 243-61 (2003).

20. Sullivan, R. M. Fossil lizards from Swain Quarry, Fort Union Formation, Middle Paleocene (Torrejonian), Carbon County, Wyoming. *J. Paleo.* **56**, 996–1010 (1982).
21. Estes, R. *Sauria Terrestria, Amphisbaenia. Handbuch der Palaoherpetologie, Part 10A.* (Gustav Fischer Verlag, Stuttgart, 1983).